Multiphoton fluorescence and second harmonic generation microscopy for imaging infectious keratitis

Hsin-Yuan Tan
Chang Gung University
College of Medicine
Chang Gung Memorial Hospital
Department of Ophthalmology
Tao Yuan, Taiwan
and
National Taiwan University
College of Medicine and College of Engineering
Institute of Biomedical Engineering
Taipei, Taiwan

Yen Sun
Wen Lo
Shu-Wen Teng
Ruei-Jr Wu
National Taiwan University
Department of Physics
Taiepei, Taiwan

Shiou-Hwa Jee
National Taiwan University
College of Medicine
National Taiwan University Hospital
Department of Dermatology
Taipei, Taiwan

Wei-Chou Lin
National Taiwan University Hospital
Department of Pathology
Taipei, Taiwan

Ching-Hsi Hsiao
Hsin-Chiung Lin
Yeong-Fong Chen
David Hui-Kang Ma
Samuel Chao-Ming Huang
Chang Gung University
College of Medicine
Chang Gung Memorial Hospital
Department of Ophthalmology
Tao Yuan, Taiwan

Sung-Jan Lin
National Taiwan University
College of Medicine
National Taiwan University Hospital
Department of Dermatology
Taipei, Taiwan
E-mail: sjlin@ha.mc.ntu.edu.tw

Chen-Yuan Dong
National Taiwan University
Department of Physics
Taipei, Taiwan
E-mail: cydong@phys.ntu.edu.tw

Abstract. The purpose of this study is to demonstrate the application of multiphoton fluorescence and second harmonic generation (SHG) microscopy for the *ex-vivo* visualization of human corneal morphological alterations due to infectious processes. The structural alterations of both cellular and collagenous components can be respectively demonstrated using fluorescence and SHG imaging. In addition, pathogens with fluorescence may be identified within turbid specimens. Our results show that multiphoton microscopy is effective for identifying structural alterations due to corneal infections without the need of histological processing. With additional developments, multiphoton microscopy has the potential to be developed into an imaging technique effective in the clinical diagnosis and monitoring of corneal infections. [DOI: 10.1117/1.2717133]

Keywords: multiphoton microscopy; second harmonic generation; cornea; infection.

Paper 06161RR received Jun. 17, 2006; revised manuscript received Jan. 11, 2007; accepted for publication Jan. 11, 2007; published online Apr. 24, 2007.

1 Introduction

Since corneal infection can lead to severe vision impairment, it is a serious condition that requires immediate medical attention. While corneal infection is a global disease, regional differences in the pathogens responsible for the infection processes do exist. In developed countries, the major predisposing factor of corneal ulcer is related to the increase in contact lens usage,[1] and in tropical countries, fungal infection may play a more significant role.[2] The timing of diagnosis and

Address all correspondence to Sung-Jan Lin or Chen-Yuan Dong.

1083-3668/2007/12(2)/024013/8/$25.00 © 2007 SPIE

application of proper antimicrobial treatment may be crucial for the clinical outcome. Currently, clinical diagnosis relies mainly on the results of cultures of corneal scrapings and biopsies. However, recalcitrant infectious keratitis may be difficult to be differentiated according to existing clinical protocols,[3–5] and an early and correct diagnosis may be crucial for selecting the appropriate antimicrobial therapy to be used. In the case of fungal infection, the diagnostic procedure usually involves more than one week of *in-vitro* culturing for identification of the responsible pathogen. Such a process can possibly delay the appropriate application of antimicrobial treatment. Therefore, an imaging technique that can provide early identification of pathogens is of great value for the clinical diagnosis of infected corneas.

Reflected confocal microscopy has been widely applied for imaging normal and diseased corneas, including infectious keratitis.[6–13] While reflected confocal microscopy can provide useful structural information of cellular components within normal and pathological corneas, it is also an effective tool for imaging the relatively large invading pathogens such as fungi and *Acanthamoeba*.[9–13] However, confocal microscopy is not effective for identifying the structural alterations of stromal collagen within infected corneas. Therefore, it is difficult to identify the extent of stromal damage from confocal imaging alone. Furthermore, the increase in corneal turbidity can lead to additional background reflection. As a result, image contrast obtained through confocal imaging can be compromised.

In recent years, multiphoton fluorescence microscopy has gained significant popularity in biomedical imaging.[14,15] The nonlinear excitation of fluorescence photons using ultrafast, near-infrared excitation sources has provided important advantages in its ability to acquire images with enhanced axial depth discrimination, reduced sample photodamage, and increased imaging penetration depths. The greatly reduced photodamage enables multiphoton fluorescence microscopy to be used in long-term observation of living cells without detectable damage.[16,17] In addition to morphological information, characteristic autofluorescence from various cells and components of the extracellular matrix can help to identify features of interest.[18,19] In addition to multiphoton fluorescence imaging, the nonlinear polarization effect from a special class of biological materials also can provide morphological information of biomedical significance. In biological structures lacking an inversion symmetry, a nonvanishing second-order susceptibility can contribute to the second harmonic generation (SHG) signal. A variety of biological materials such as collagen, muscle fibers, and microtubules have been shown to be effective in generating second harmonic signals.[19–23] Specifically, collagen is a particularly interesting structure for SHG imaging due to the fact that it is widely distributed in extracellular matrices of various tissues, including the cornea. The combination of multiphoton fluorescence and the SHG technique in biological imaging has been applied in medicine, including dermatology and ophthalmology.[24–26] Previously, the application of multiphoton fluorescence and SHG microscopy in mapping spectrally resolved morphological features of the cornea has been demonstrated.[27] It was found that the corneal epithelium is strongly autofluorescent and no SHG signals can be detected within the epithelial layer. Since cellular autofluorescence comes largely from NAD(P)H and the nucleus is devoid of NAD(P)H, halo-like structures with dark central regions may be identified as epithelial cells.[28] In addition, SHG images of normal corneal stroma showed regular distribution patterns of collagen fibers. The inability to image keratocytes suggests that normal quiescent keratocytes are less fluorescent than corneal epithelial cells. In addition to imaging the normal cornea, it was found that quantitative SHG microscopy is effective in characterizing the temperature-related collagen changes in porcine corneas.[29] In this work, we extend the applications of multiphoton fluorescence and SHG microscopy for imaging corneal infection from the various pathogens of bacteria, fungus, and *Acanthamoeba*. We hope to demonstrate the potential of multiphoton microscopy as a noninvasive diagnostic and monitoring tool for corneal infections in clinical applications.

2 Materials and Methods

The study protocol was approved by an institutional review board and informed consent has been obtained from the patients. We conformed to the Helsinki Declaration with respect to human subjects in biomedical research. The infected human corneal samples with culture-proven pathogens were obtained from surgical procedures. The trephined corneal buttons were placed on slides and flattened with coverslips for imaging. All the imaging procedures were performed at room temperature and completed within 12 h after surgery.

The multiphoton fluorescence and SHG microscopic system used in this study is similar to the system previously described.[27,29] A diode-pumped solid state (Millennia X, Spectra Physics, Mountain View, California), titanium-sapphire laser (Ti:sapphire Tsunami, Spectra Physics) was used as the excitation source. The 760-nm output of the Ti:sapphire laser is scanned in the focal plane by a galvanometer-driver *x-y* mirror scanning system (Model 6220, Cambridge Technology, Cambridge, Massachusetts). For high resolution imaging, high-numerical-aperture water immersion objectives (Fluor 40×, NA 0.8, Nikon; Fluor 20×, NA 0.8, Nikon) were used. The SHG signal centered at 380 nm was reflected by the secondary dichroic, and further filtered using a bandpass filter (HQ380/20, Chroma Technology), while the longer wavelength fluorescence passed through the dichroic mirror and a filter (E435LP, Chroma Technology) before being detected. For large area scan of the corneal specimens, a stage scanning system (H101, Prior Scientific, United Kingdom) was used for specimen translation. After imaging, the specimens were further processed for histological examination for comparison.

To quantify the structural information obtained both from fluorescence and SHG signals, we adopted the index that was previously applied for quantifying aging change of skin (SAAID) to evaluate the structural destruction within infected stroma.[30] Briefly, the number of SHG pixels within each image are defined as a, that pixels of the multiphoton fluorescence area image is defined as b. Finally, the SAAID is defined as $(a-b)/(a+b)$. The index of SAAID decreases as the SHG area decreases, which represents the destruction of collagenous stroma during the infectious process.

3 Results

To investigate the possibility of characterizing the extent of structural damage and to identify the pathogens within infected corneas, we performed *ex-vivo* multiphoton imaging on

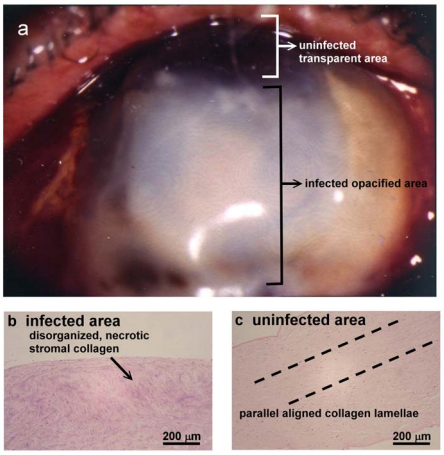

Fig. 1 (a) The clinical photography of *Serratia marcescens* keratitis. A large ulcerated, turbid stroma with dense infiltration can be identified. Only a small part of the cornea at the upper portion remains clear and unaffected. (b) The histological image taken from the ulcerated area of a corneal specimen. The normal parallel aligned collagen lamellae was altered within infected stroma, and replaced with irregularly packed necrotized collagen structure. (c) The histological image taken from the relatively optical clear region of a corneal specimen. The normal parallel aligned collagen lamellae remain within the uninfected area.

three corneas with culture-proven infections from the bacterium (*Serratia marcescens*), fungus (*Alternaria sp.*), and *Acanthamoeba castellanii* with coinfection of *Pseudomonas aeruginosa*. Our multiphoton images are compared with histological results and are presented next.

3.1 *Ex-Vivo Multiphoton Imaging of Bacterial Keratitis (Serratia marcescens)*

The first infected cornea we present was obtained from a 72-year-old male who experienced redness and pain in his post-keratoplastic left eye. A large central ulceration with dense stromal infiltration was noted on arrival [Fig. 1(a)]. Corneal scraping was performed for laboratory examination, and empirical antibiotic treatment was prescribed immediately. *Serratia marscecens* growth was identified days later, and despite medical treatment, stromal melting continued. Due to the threat of perforation, therapeutic penetrating keratoplasty was performed one week later. The removed cornea specimen was sent for multiphoton examination.

The combined fluorescence and SHG images of the specimen are shown in Figs. 2 and 3, and the histological image is shown in Figs. 1(b) and 1(c) for comparison. At the surface of the ulcerated region [Fig. 2(a)], no corresponding fluorescent epithelial cells can be identified, which is compatible with histological findings [Fig. 1(b)]. In addition, unlike the normal stroma, which is composed largely of a regular pattern of SHG collagen fiber network with minimal fluorescence signal, significant increase of fluorescent clusters in the background can be identified within Fig. 2(a). To illustrate additional features within the large-area image, magnified images from selected regions of interest are shown in Figs. 2(b) and 2(c). In these images, infiltration of round inflammatory cells can be identified within the turbid, infected area [Fig. 2(b)], and increased fluorescence in the background was detected in areas lacking SHG signals [Fig. 2(c)]. Furthermore, we compared the multiphoton image of the infected area [Fig. 3(a)] to that of the relatively uninfected area [Fig. 3(b)] at the depth of

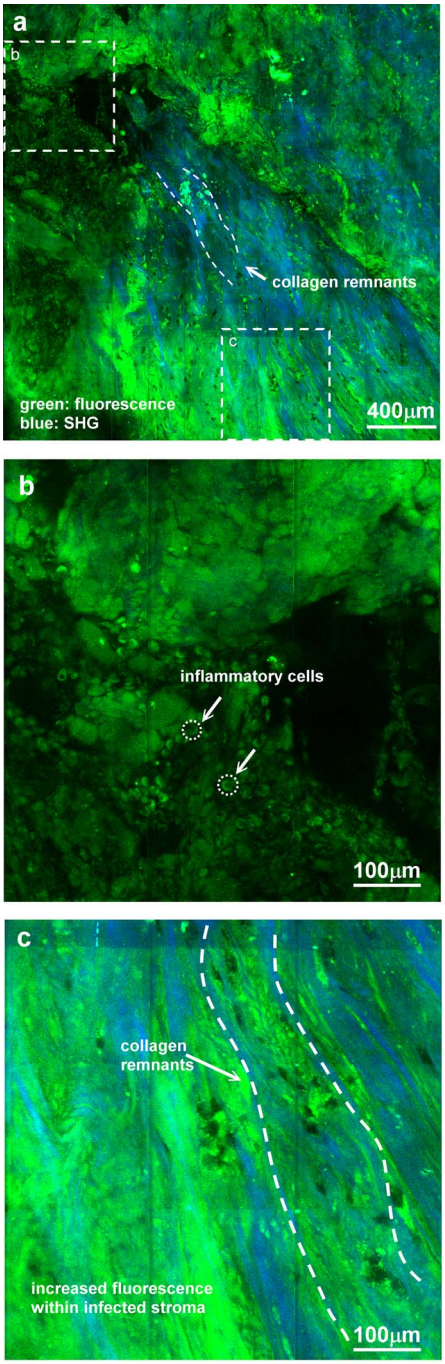

Fig. 2 The multiphoton images of *Serratia marcescens* keratitis. (a) The large-scale image taken at the surface of the ulcerated area of the corneal specimen. The infected stroma is composed of irregularly distributed fluorescent signals and collagen remnants. The detailed images from areas b and c in (a) are displayed in (b) and (c), respectively. Infiltration of fluorescent inflammatory cells within infected stroma can be seen in detailed image (b). The collagen remnants identified with SHG signals was observed in (c).

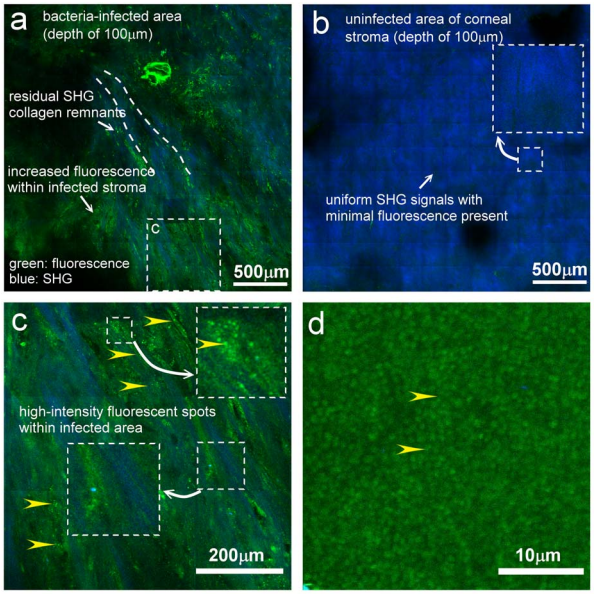

Fig. 3 The multiphoton images of *Serratia marcescens* keratitis. (a) The image taken at the ulcerated area at the depth of 100 μm. The infected stroma is found to be composed of irregularly distributed fluorescent signals and collagen remnants. (b) The image taken at the optical clear area at the same depth. On the other hand, the uninfected stroma is composed mainly of uniformly distributed SHG signals, with minimal fluorescent signal present. (c) The detailed image from area c in (a). Fluorescent spots (yellow arrowheads), possibly due to the infecting bacteria, were visualized. (d) The multiphoton image from isolated *Serratia marcescens* taken from a colony. Autofluroescent bacteria can be visualized (yellow arrowheads, color online only).

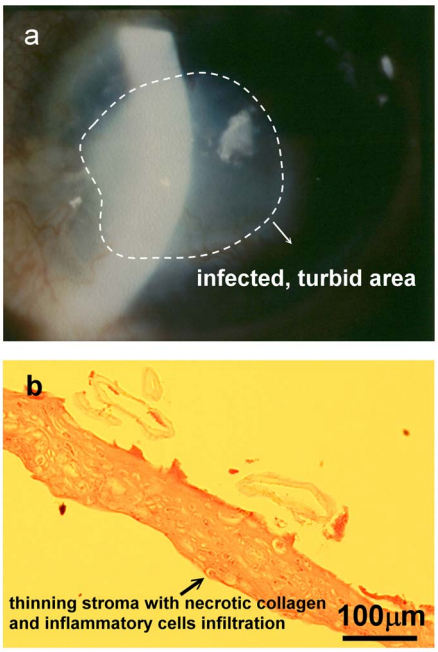

Fig. 4 (a) Clinical photography of the *Alternaria* keratitis case. Central ulceration and turbid stroma can be identified. (b) The histological image taken from the corneal specimen. Thinning of corneal stroma and destruction of normal parallel aligned collagen lamellae can be visualized.

100 μm from the surface. In the infected area, significant increase of fluorescence in the background as well as irregularly aligned SHG signals can be observed, while in the less infected area, a homogenous distribution of SHG collagen within the stroma can be identified. Moreover, a comparision of the multiphoton images of purified *Serratia marscecens* in suspension [Fig. 3(d)] with a detailed image of the infected area [Fig. 3(c)] suggests that the high-intensity fluorescent spots [yellow arrows in Figs. 3(c) and 3(d)] may be the infiltrated bacteria, although further investigation is needed to confirm this hypothesis.

3.2 *Ex-Vivo Multiphoton Imaging of Fungal Keratitis (Alternaria sp.)*

The second sample we present was obtained from a 70-year-old female patient who experienced eye pain in her left eye for days. On arrival, a large central ulceration was noted [Fig. 4(a)]. The suspicion of fungal infection led to the immediate prescription of topical natamycin 10%. Eventually, superficial keratectomy was performed to eradicate the lesion. One week later, laboratory examinations revealed that the fungus *Alternaria sp.* was the responsible pathogen. The trephined corneal specimen was then sent for multiphoton examination immediately, and histological examination was performed for comparison [Fig. 4(b)].

The large-scale multiphoton image is shown in Fig. 5(a). Similar to the case of bacterial infection, fluorescence within the stroma markedly increased. The patterns of increased fluorescent signals and remaining SHG signals are distributed in parallel, crossed patterns [Figs. 5(b) and 5(c)], similar to that found within the less affected stroma of *Serratia marcescens* keratitis [Fig. 3(b)]. Similar to the bacterial keratitis case, the SHG signals from stromal collagen diminished. In both the large scale [Fig. 5(a)] and magnified images [Fig. 5(d)], tube-like structures can be identified. Comparison with the multiphoton image of purified *Alternaria* [Fig. 5(e)] suggests that these structures are most likely the hyphae of the infecting fungus.

3.3 *Ex-Vivo Multiphoton Imaging of Acanthamoeba castellinii Keratitis (Coinfection with Pseudomonas aeruginosa)*

The third specimen we present was obtained from a 12-year-old male who suffered from severe eye pain in his right eye for days. No significant trauma history was recalled except for the regular wearing of overnight vision-correcting orthokeratology lenses. Large ring-shaped infiltration was noted in his right eye on arrival. Since *Acanthamoeba* infection was suspected, intensive antimicrobial treatment was applied, and cultures were performed after the patient was admitted. Days later, the culture result revealed the coinfection of *Acanthamoeba castellinii* and *Pseudomonas aeruginosa*. Despite medical treatment, the infection aggravated [Fig. 6(a)]. To achieve a complete eradication of the pathogens, therapeutic penetrating keratoplasty was performed. The specimen was then sent for multiphoton imaging and later processed for histological examination [Fig. 6(b)].

In the large scale image shown in Fig. 7(a), fluorescent

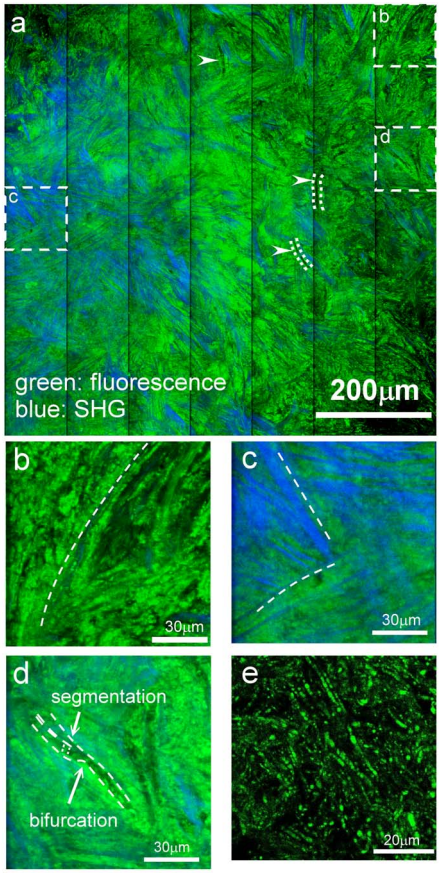

Fig. 5 The multiphoton images of *Alternaria* keratitis. (a) The large-scale image taken at the surface of the ulcerated area of a corneal specimen. (b), (c), and (d) The magnified image of areas b, c, and d, respectively. The infected stroma is found to be composed of fluorescent signals and irregularly distributed collagen remnants (a). Parallel distributed fluorescence in the background and residual SHG-generating collagen remnants were found in images (b) and (c). Possible fungal hyphae with characteristic morphology of bifurcation and segmentation can be visualized both in the large-scale and detailed images (white arrows) (a) and (d). (e) Multiphoton imaging of *Alternaria sp.*

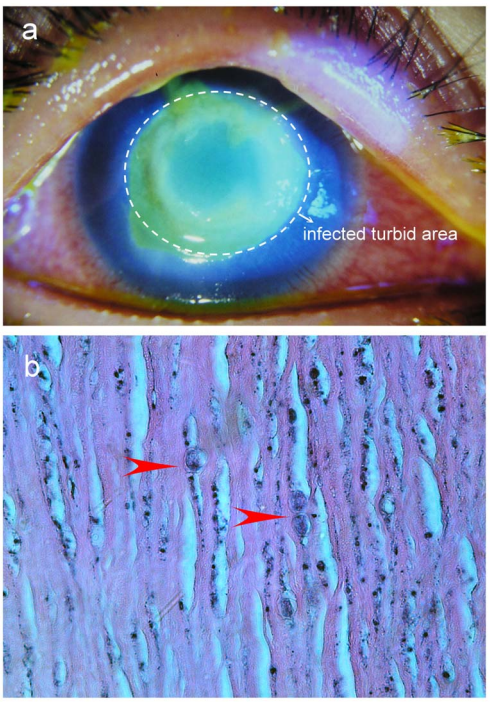

Fig. 6 (a) The clinical photography of *Acanthamoeba* keratitis. Large central ulcerated stroma lacking of epithelium can be demonstrated with fluorescein staining. (b) The histological picture taken from the corneal specimen. The *Acanthamoeba* cysts can be identified within stroma (red arrowheads).

Acanthamoeba cysts (yellow arrowheads) as well as fluorescent bacilli (red arrow) can be identified within the infected corneal stroma. Compared to the less infected stroma [Fig. 3(b)], Fig. 7(a) shows a markedly increased fluorescence level, which may represent the pathological destruction of corneal stroma. The decrease of normal stromal collagen responsible for the SHG signals and the increase in fluorescence indicate the destruction of stromal structure during the infection process. While second harmonic generating collagen fibers can still be found [Fig. 7(d)], the responsible structures lack the regular collagen organization found within the less infected stroma.

Our results suggest that during the infection process, the normal, regularly organized stromal architecture has been adversely altered. In addition, fluorescent *Acanthamoeba* cysts and bacilli can be identified within the turbid stroma. In the detailed images, in addition to the observation of fluorescent *Acanthamoeba* cysts [Fig. 7(c), yellow arrowhead], individual spots can also be visualized with fluorescence [Fig. 7(b), red arrowhead]. Comparison with the multiphoton image of isolated *Pseudomonas aeruginosa* [Fig. 7(e)] suggests that these spots are the individual bacteria.

In addition, we also found *Acanthamoeba* cysts within the less affected area with preserved collagen structure demonstrated by SHG signals and minimal infiltration of inflammatory cells [Fig. 7(d), yellow arrowhead], which may implicate the possible residence of quiescent *Acanthamoeba* cysts within the clinically clear area. This observation may be helpful for designing treatment strategy at the late stages of infection.

The indices of SAAID (ratio of the difference and sum of the SHG and fluorescence areas) from three representative infectious cases are shown in Table 1. For the infected cornea specimens due to *Serratia marscecens* and *Acanthamoeba-Pseudomonas aeruginosa*, the respective SAAID values of −0.25 and −0.60 were obtained. On the other hand, the SAAID ratios for the less infected *Serratia marscecens* and *Alternaria* cases were −0.02. These results suggest that the SAAID ratio may be used to characterize the extent of corneal damage in cases of infectious keratitis.

4 Discussion

Infectious keratitis is of great significance in clinical practice. It is one of the major causes responsible for visual loss. A rapid clinical diagnosis sometimes can be difficult, and the delay in diagnosis can hinder appropriate treatment to be applied. In addition, during the later stages of treatment, it is

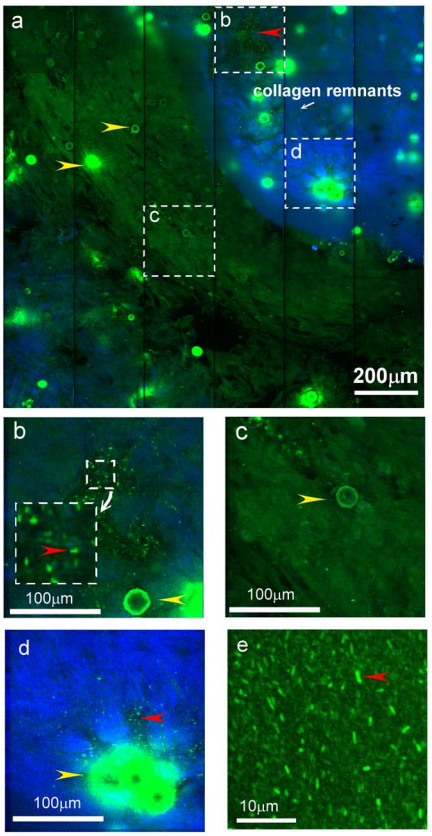

Fig. 7 The multiphoton images of *Acanthamoeba* keratitis. (a) The large-scale image taken at the ulcerated area of the corneal specimen. (b), (c), and (d) Detailed images from areas b, c, and d in (a). *Acanthamoeba* cysts (yellow arrowheads) and *Pseudomonas* bacteria (red arrowheads) were identified with fluorescence. (e) The image of isolated *Pseudomonas aeruginosa* from a colony.

often difficult to evaluate the tissue response to treatment. The turbid cornea caused by infectious processes may hinder the clinical evaluation of disease progression. Sometimes the drug-related toxic effect may be difficult to be differentiated from the subtle exacerbation of infection or the retardation of wound healing due to coexisting inflammation.[31] In the case of fungal and *Acanthamoeba* infections, clinical consequences are usually longer and easily relapsed if traces of pathogens remain within the cornea. In less certain cases, repeated biopsies may sometimes be necessary for deciding on a treatment strategy. Yet the threat of perforation is always a concern. Therefore, the development of a noninvasive *in-vivo* monitoring system for the detection of pathogens and the extent of destruction may be beneficial in cases of recalcitrant infections.

Table 1 The indices of SAAID from three representative infectious cases. The definition of the SAAID index is the size difference between the area with SHG signals and the area with autofluorescence, divided by their sum (SHG−AF)/(SHG+AF). These ratios may be used to characterize the extent of corneal damage during infectious processes.

Group	SAAID index
Infected with *Serratia marcescens*	−0.25
Less infected area in the sample infected with *Serratia marcescens*	−0.02
Infected with *Alternaria sp.*	−0.02
Coinfected with *Acanthamoeba castellanii and Pseudomonas aeruginosa*	−0.60

In our work, we successfully demonstrated the *ex-vivo*, multiphoton fluorescence and SHG imaging for visualizing infectious keratitis caused by various pathogens of *Serratia marscecens*, *Alternaria*, and *Acanthamoeba-Pseudomonas aeruginosa*. In our previous work, we had demonstrated that in a normal cornea, the cellular architecture of the corneal epithelium can be visualized with fluorescence microscopy, while the stromal collagen can be visualized using SHG imaging. Under normal physiological conditions, the quiescent keratocytes are ineffective in generating fluorescence. Here we further demonstrated both the structural alterations of cellular and collagenous components of the cornea without the need of additional sample processing procedures. First, we found the absence of fluorescent epithelial cells, which is compatible with the histological findings of epithelial defects in ulcerated cornea. In the infected stroma, we found disorganized or absent SHG signals within the infected areas, which may correspond to the destruction or regeneration of stromal collagen during infection processes. The altered turbid stroma of the inflamed cornea may sometimes be difficult to be differentiated by clinical observations. Our results show that multiphoton imaging has the potential to monitor the destruction and the regeneration of stromal collagen. In regions with more severe stromal damage, the SHG signal may be greatly diminished or absent when collagen structures are altered. This feature may provide important information in deciding the treatment strategy in the late wound healing stage of corneal infection. We also found that increased fluorescence can be observed in the infected stroma, especially within regions lacking SHG signals. Even with significant background fluorescence, inflammatory cells can still be observed. The exact nature of the increased fluorescence signals in the infected cornea is unknown at this point. There are several possible origins of the fluorescence signals. One possibility is that the fluorescence came from the degenerated collagen. It has been shown that fluorescence signals increase in thermally treated dermis where collagen is denatured.[32] Another explanation for the increased fluorescence is that fluorescent substances can be released by the causative agents during the infection process. It is likely that inflammatory cells may also contribute to fluorescence signals. The exact mechanism contributing to the increased fluorescence during infection processes needs further investigation.

An important advantage of multiphoton microscopy in diagnosing corneal keratitis is the identification of infecting pathogens. Our results suggest that bacteria, fungi, and *Acanthamoeba* cysts within corneal specimens may be visualized without additional histological processing. Therefore, multiphoton imaging may be effective for real-time detection of pathogens at early stages of infection, and for detecting re-

sidual recalcitrant pathogens such as fungi and *Acanthamoeba* in the late stage of infection. Therefore, multiphoton microscopy may provide information for on-the-spot determination of treatment strategy. In addition, the spectral properties of different pathogens may be investigated for more precise identification.

Due to the limited cases available to us, we were not able to investigate the effects of age on corneal infection. Aging has been demonstrated to affect the infectious process by influencing the immune reaction.[33] In addition, normal stromal architecture has been proven to be altered during the aging process. Specifically, it was found that the number of collagen fibers, interfibrillar spacing, and the degree of cross-linking all increased with age.[34] However, the destruction of corneal architecture that we observed in the keratitis specimens does not correlate with age-related changes. Therefore, the conclusions reached by our study are most likely unaffected by the age of the cornea specimen. Since the interplay of host tissue and invading pathogens is a complex phenomenon, future studies of corneal keratitis should systematically investigate the effects on the corneas from parameters such as patient age and the duration of infection. This work merely demonstrates the potential of multiphoton microscopy in investigating the physiological changes associated with corneas due to infectious keratitis.

In conclusion, we demonstrated that multiphoton fluorescence and SHG microscopy can be used for the characterization of morphological alterations in corneal infections and as an effective diagnostic tool for pathogen detection. With additional development, multiphoton imaging may be developed into a noninvasive diagnostic and monitoring system for corneal infections, and can potentially be applied to studying infectious processes of other tissues.

Acknowledgment

This study was supported in part by the National Research Program for Genomic Medicine (NRPGM), Taiwan (NSC93-3112-B-002-033 and NSC93-3112-B-002-034), and was completed in the Optical Molecular Imaging Microscopy Core Facility (A5) of NRPGM. We also like to thank Chiu-Mei Hsueh for helping with image processing.

References

1. J. Dart, F. Stapleton, and D. Minassian, "Contact lenses and other risk factors in microbial keratitis," *Lancet* **338**, 650–653 (1991).
2. E. Huang, D. Lam, D. Fan, and D. Seal, "Microbial keratitis in Hong Kong: relationship to climate, environment and contact-lens disinfection," *Trans. R. Soc. Trop. Med. Hyg.* **95**, 361–367 (2001).
3. P. A. Thomas, "Fungal infections of the cornea," *Eye* **17**, 852–862 (2003).
4. A. S. Bacon, D. G. Frazer, J. K. Dart, M. Matheson, L. A. Ficker, and P. A. Wright, "Review of 72 consecutive cases of Acanthamoeba keratitis, 1984-1992," *Eye* **7**, 719–725 (1993).
5. C. F. Radford, D. C. Minassian, and J. K. Dart, "Acanthamoeba keratitis in England and Wales: incidence, outcome, and risk factors," *Br. J. Ophthamol.* **86**, 536–542 (2002).
6. H. D. Cavanagh, W. M. Petroll, and A. H. Alizadeh, "Clinical and diagnostic use of in vivo confocal microscopy in patients with corneal disease," *Ophthalmology* **100**, 1444–1454 (1993).
7. I. Jalbert, F. Stapleton, E. Papas, D. F. Sweeney, and M. Coroneo, "In vivo confocal microscopy of the human cornea," *Br. J. Ophthamol.* **87**, 225–236 (2003).
8. S. J. Chew, R. W. Beuerman, M. Assouline, H. E. Kaufman, B. A. Barron, and J. M. Hill, "Early diagnosis of infectious keratitis with in vivo real time confocal microscopy," *CLAO J.* **18**, 197–201 (1992).
9. K. Winchester, W. D. Mathers, and J. E. Sutphin, "Diagnosis of Aspergillus keratitis in vivo with confocal microscopy," *Cornea* **16**, 27–31 (1997).
10. G. J. Florakis, G. Moazami, H. Schubert, C. J. Koester, and J. D. Auran, "Scanning slit confocal microscopy of fungal keratitis," *Arch. Ophthalmol. (Chicago)* **115**, 1461–1463 (1997).
11. A. M. Avunduk, R. W. Beuerman, E. D. Varnell, and H. E. Kaufman, "Confocal microscopy of Aspergillus fumigatus keratitis," *Br. J. Ophthamol.* **87**, 409–410 (2003).
12. D. R. Pfister, J. D. Cameron, J. H. Krachmer, and E. J. Holland, "Confocal microscopy findings of Acanthamoeba keratitis," *Am. J. Ophthalmol.* **121**, 119–128 (1996).
13. S. C. Kaufman, J. A. Laird, R. Cooper, and B. W. Beuerman, "Diagnosis of bacterial contact lens related keratitis with the white-light confocal microscope," *CLAO J.* **22**, 274–277 (1996).
14. W. Denk, J. H. Strickler, and W. W. Webb, "Two-photon laser scanning fluorescence microscopy," *Science* **248**, 73–76 (1990).
15. P. T. C. So, C. Y. Dong, B. R. Masters, and K. M. Berland, "Two-photon excitation fluorescence microscopy," *Annu. Rev. Biomed. Eng.* **2**, 399–429 (2000).
16. J. M. Squirrell, D. L. Wokosin, J. G. White, and B. D. Bavister, "Long-term two-photon fluorescence imaging of mammalian embryos without compromising viability," *Nat. Biotechnol.* **17**, 763–767 (1999).
17. M. J. Miller, S. H. Wei, I. Parker, and M. D. Cahalan, "Two-photon imaging of lymphocyte motility and antigen response in intact lymph node," *Science* **296**, 1869–1873 (2002).
18. W. R. Zipfel, R. M. Williams, and W. W. Webb, "Nonlinear magic: multiphoton microscopy in the biosciences," *Nat. Biotechnol.* **21**, 1369–1377 (2003).
19. W. R. Zipfel, R. M. Williams, R. Christie, A. Y. Nikitin, B. T. Hyman, and W. W. Webb, "Live tissue intrinsic emission microscopy using multiphoton-excited native fluorescence and second harmonic generation," *Proc. Natl. Acad. Sci. U.S.A.* **100**, 7075–7080 (2003).
20. A. Zoumi, A. Yeh, and B. J. Tromberg, "Imaging cells and extracellular matrix in vivo by using second-harmonic generation and two-photon excited fluorescence," *Proc. Natl. Acad. Sci. U.S.A.* **99**, 11014–11019 (2002).
21. A. Zoumi, X. Lu, G. S. Kassab, and B. J. Tromberg, "Imaging coronary artery microstructure using second-harmonic and two-photon fluorescence microscopy," *Biophys. J.* **7**, 2778–2786 (2004).
22. P. J. Campagnola and L. M. Loew, "Second-harmonic imaging microscopy for visualizing biomolecular arrays in cells, tissues and organisms," *Nat. Biotechnol.* **21**, 1356–1360 (2003).
23. E. Brown, T. McKee, E. diTomaso, A. Pluen, B. Seed, Y. Boucher, and R. K. Jain, "Dynamic imaging of collagen and its modulation in tumors in vivo using second-harmonic generation," *Nat. Med.* **9**, 796–800 (2003).
24. B. R. Masters, P. T. C. So, and E. Gratton, "Multiphoton excitation fluorescence microscopy and spectroscopy of in vivo human skin," *Biophys. J.* **72**, 2405–2412 (1997).
25. Y. Sun, J. W. Su, W. Lo, S. J. Lin, S. H. Jee, and C. Y. Dong, "Multiphoton polarization imaging of the stratum corneum and the dermis in ex-vivo human skin," *Opt. Express* **11**, 3377–3384 (2003).
26. A. T. Yeh, N. Nassif, A. Zoumi, and B. J. Tromberg, "Selective corneal imaging using combined second-harmonic generation and two-photon excited fluorescence," *Opt. Lett.* **27**, 2082–2084 (2002).
27. S. W. Teng, H. Y. Tan, J. L. Peng, H. H. Lin, K. H. Kim, W. Lo, Y. Sun, W. C. Lin, S. J. Lin, S. H. Jee, P. T. C. So, and C. Y. Dong, "Multiphoton autofluorescence and second-harmonic generation (SHG) imaging of ex-vivo porcine eye," *Invest. Ophthalmol. Visual Sci.* **47**, 1216–1224 (2006).
28. D. W. Piston, B. R. Masters, and W. W. Webb, "Three-dimensionally resolved NAD(P)H cellular metabolic redox imaging of the in situ cornea with two-photon excitation laser scanning microscopy," *J. Microsc.* **178**, 20–27 (1995).
29. H. Y. Tan, S. W. Teng, W. Lo, W. C. Lin, S. J. Lin, S. H. Jee, and C. Y. Dong, "Characterizing the thermally induced structural changes to intact porcine eye, part 1: second harmonic generation imaging of cornea stroma," *J. Biomed. Opt.* **10**(5), 054019 (2005).
30. S. J. Lin, R. J. Wu, H. Y. Tan, W. Lo, W. C. Lin, T. H. Young, C. J. Hsu, J. S. Chen, S. H. Jee, and C. Y. Dong, "Evaluating cutaneous photoaging by use of multiphoton fluorescence and second harmonic generation microscopy," *Opt. Lett.* **30**(17), 2275–2277 (2005).

31. B. D. Allan and J. K. Dart, "Strategies for the management of microbial keratitis," *Br. J. Ophthamol.* **79**, 777–786 (1995).
32. L. T. Vo, P. Anikijenko, W. J. McLaren, P. M. Delaney, D. H. Barkla, and R. G. King, "Autofluorescence of skin burns detected by fiber-optic confocal imaging: evidence that cool water treatment limits progressive thermal damage in anesthetized hairless mice," *J. Trauma: Inj., Infect., Crit. Care* **51**, 98–104 (2001).
33. K. A. Kernacki, R. P. Barrett, S. A. McClellan, and L. D. Hazlett, "Aging and PMN response to P. aeruginosa infection," *Invest. Ophthalmol. Visual Sci.* **51**, 3019–3025 (2000).
34. N. S. Malik, S. J. Moss, N. Ahmed, A. J. Furth, R. S. Wall, and K. M. Meek, "Aging of the human corneal stroma: structural and biochemical changes," *Biochim. Biophys. Acta* **1138**, 222–228 (1992).